

# The salinity: $\delta^{18}\text{O}$ water relationship in Kongsfjorden, western Spitsbergen

Suzanne E. MacLachlan,<sup>1</sup> Finlo R Cottier,<sup>1</sup> William E. N. Austin<sup>2</sup> & John A. Howe<sup>1</sup>

<sup>1</sup> Scottish Association for Marine Science, Dunstaffnage Marine Laboratory, Argyll, Oban, PA37 1QA, UK

<sup>2</sup> School of Geography and Geosciences, University of St Andrews, Fife, KY16 9AL, UK

## Keywords

oxygen isotopes; mixing line; Arctic; fjord; glacial; hydrography.

## Correspondence

Suzanne MacLachlan, Geology and Geophysics, National Oceanography Centre, University of Southampton, European Way, Southampton, SO14 3ZH, UK. E-mail: sucl@noc.soton.ac.uk.

doi:10.1111/j.1751-8369.2007.00016.x

## Abstract

We present the first oxygen isotope measurements from Kongsfjorden in north-west Spitsbergen, and use the isotopic composition and hydrographic data to provide a detailed assessment of the mixing between freshwater and oceanic waters. Temperature, salinity(s) and oxygen isotope profiles are used to describe the seasonal evolution of hydrography in the inner part of the fjord, and to infer the dominant mixing and exchange processes. Data from atmospheric, glacial and marine sources throughout Kongsfjorden are used to construct a salinity:  $\delta^{18}\text{O}$  mixing line in a region that receives inputs of freshwater and marine Atlantic water. The dominant source of freshwater is glacial melt from a tidewater glacier complex at the head of the fjord, resulting in a seawater salinity:  $\delta^{18}\text{O}$  relationship where  $\delta^{18}\text{O} = 0.43S - 14.65$ . The Kongsfjorden data provides a northern latitudinal limit for mixing lines in the north-western European coastal system.

The marine environment of western Svalbard is strongly influenced by the West Spitsbergen Current (WSC), the northern extension of the Norwegian Atlantic Current. The WSC follows the slope to the west of Svalbard delivering relatively warm and saline Atlantic water (AW) northwards, and is the main transport of heat to the Arctic (Schauer et al. 2004). Colder and less saline water of Arctic origin flows along the West Spitsbergen Shelf (WSS), where an oceanic front develops with the WSC (Saloranta & Svendsen 2001). Consequently, the WSS is a location characterized by considerable exchange and mixing of Atlantic and Arctic waters and fjordic freshwater.

Glaciated Arctic fjords are typically characterized by linear environmental gradients. Tidewater glaciers at the head of these fjords discharge freshwater and suspended sediment into the inner parts of the fjord, whereas predominantly marine conditions prevail at the fjord mouth (cf. Freeland et al. 1980 in Syvitski et al. 1984). Wind, tidal and geostrophic forces in such fjords can generate complex layering and mixing between water masses (Svendsen et al. 2002).

A recent study of Kongsfjorden, Spitsbergen, by Cottier et al. (2005) described the intense seasonality, characterized by a fundamental shift in hydrographic conditions. A somewhat homogeneous water mass is created in winter

through the processes of convection and sea-ice formation. In summer, frontal instabilities at the shelf break result in the intrusion of AW into the fjord. The volume of such intrusions varies interannually, and the controlling parameters include the magnitude and direction of shelf winds during spring and summer, and the relative density structure between the shelf and fjord waters.

The application of oxygen isotope measurements for differentiating between meteoric and sea-ice meltwater has been thoroughly demonstrated (Craig & Gordon 1965; Bedard et al. 1981; Bauch et al. 1995). The latitudinal variation in the value of  $\delta^{18}\text{O}$  for meteoric water, caused by temperature and distance from the evaporation site, makes  $\delta^{18}\text{O}$  an ideal tracer to identify high-latitude freshwater sources. Finally, salinity:  $\delta^{18}\text{O}$  mixing lines are particularly valuable in high-latitude locations, as they can be used to trace and identify the mechanism associated with deep water formation (Bauch et al. 2005).

The oxygen isotope ratios in fossil carbonate buried in marine sediments are considered to reflect the ratios prevailing in the ocean at the time of burial. The stable oxygen isotope ratio within calcareous organisms (such as foraminifera, molluscs, ostracods etc.) is a function of (i) the isotopic composition of the sea water, and (ii) the temperature of the water (e.g. Jansen 1989). In

particular, species that calcify their shells in isotopic equilibrium with the ambient water, or where the isotopic vital effect is known, are the most useful as palaeoceanographic indicators. A comprehensive understanding of the salinity and  $\delta^{18}\text{O}$  properties of the encompassing water masses is therefore essential in quantifying the temperature and salinity effects encoded within the stable oxygen isotope record of calcareous organisms.

A study by Azetsu-Scott & Tan (1997) investigated the dynamics of a surface glacial meltwater plume in Kangerdlugssuaq fjord, East Greenland, using oxygen isotopes as a tracer. A linear relationship between salinity and  $\delta^{18}\text{O}$  confirmed the dominant source of freshwater in the fjord to be of glacial origin. Oxygen isotope mixing lines have also been constructed for Sognefjorden, western Norway (Mikalsen & Sejrup 2000), showing a large gradient in the oxygen isotope composition from the fjord head ( $-14.5\text{‰}$ ), increasing westward to the fjord mouth ( $-9.2\text{‰}$ ), with a mixing line of  $0.31\text{‰}$  per unit salinity change.

Previous oceanographic investigations in Kongsfjorden by Svendsen et al. (2002) and Cottier et al. (2005), were

focused on the modification and exchange of the water masses in the outer fjord and on the adjacent shelf. For a more complete understanding of the water mass distribution within this and similar fjords, it is also important to consider the interactions between atmosphere, ocean, glacial ice and sea ice. Stable isotopes can be employed to distinguish the influence of these processes on modifying the different water masses within glaciated fjords. This study investigates how mixing between oceanic, coastal and catchment waters influence the oxygen isotope composition in an Arctic fjord. Furthermore, the study provides data that can be utilized as a calibration tool for regional palaeoceanographic research in fjordic environments.

### Regional setting

The Kongsfjorden–Krossfjorden system is situated between  $78^{\circ} 04' \text{N}$  and  $79^{\circ} 03' \text{N}$ , and  $11^{\circ} 03' \text{E}$  and  $13^{\circ} 3' \text{E}$  (Fig. 1). Kongsfjorden is orientated south-east to north-west, is approximately 20 km long and varies from 4 to 10 km wide, and has a complex bottom topography

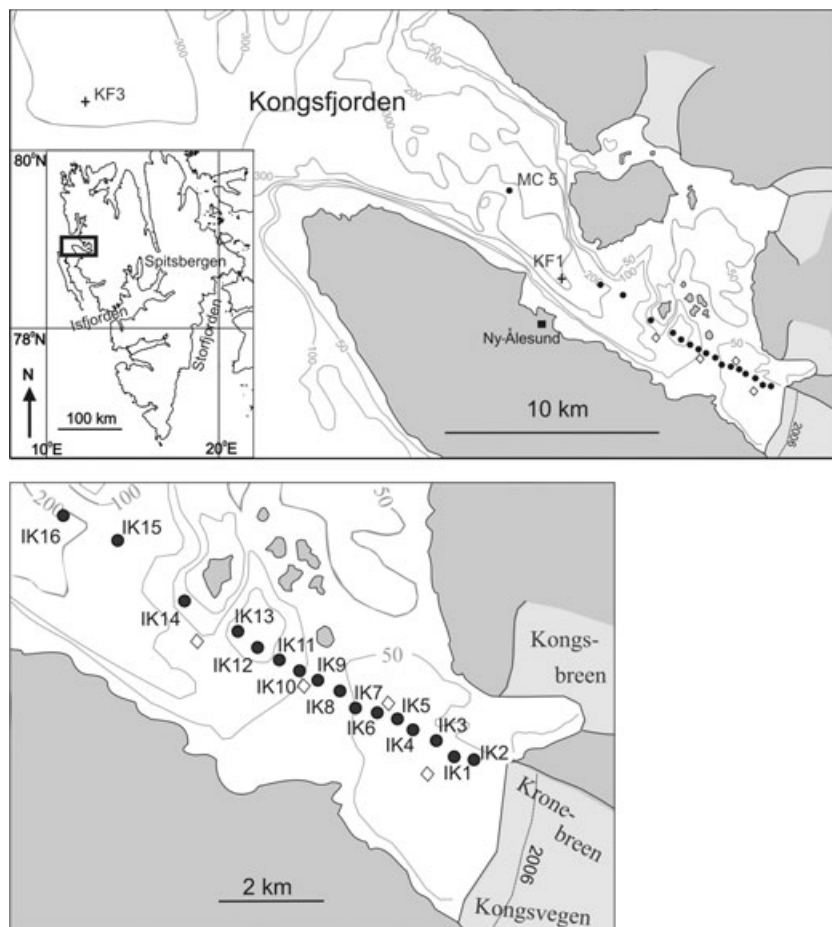


**Fig. 1** Location and station map of Kongsfjorden. We define the outer fjord as the area north-west of Ny-Ålesund. +, July 2002 (cruise JR75); filled circles indicate sites used in September 2005 (cruise JR127); open diamonds indicate sites used between 30 March and 3 April 2005 (ice stations).

comprising of a number of sills and basins (Howe et al. 2004). Throughout the paper we subdivide the fjord into the inner fjord (south-east of Ny-Ålesund) and the outer fjord (north-west of Ny-Ålesund). The fjord has a distinct deep-water connection (at a depth of approximately 350 m) to the adjacent shelf. The dynamic character of the fjord-shelf region (Saloranta & Svendsen 2001) permits seasonal inflow of shelf and oceanic water masses, which impact on the hydrographic (Cottier et al. 2005) and biological characteristics of the fjord (Willis et al. 2006).

Circulation in Kongsfjorden is dominated by cyclonic currents resulting from the reduced Rossby radius by virtue of the high-latitude location (Ingvaldsen et al. 2001). The magnitude of transverse salinity gradients in the fjords is not static but undergoes constant adjustment by the prevalence and strength of the axial fjord winds. Fast ice begins to form in the inner fjord during December/January, reaching a total thickness of up to 1 m, and can break up to form drift ice in the outer fjord. Loss of sea ice from the fjord is primarily the result of break-up by waves and down-fjord winds, rather than by local melting (Svendsen et al. 2002).

There is an active tidal glacier complex at the head of the fjord that generates steep environmental gradients in salinity, temperature, sedimentation rates and bottom sediment composition (Svendsen et al. 2002). The catchment area has been estimated as 1260 km<sup>2</sup>, and approximately 80% of it was reported to be glaciated (Ito & Kudho 1997). Kongsvegen and Kronebreen are tidewater glaciers at the head of Kongsfjorden, and together drain an area of 1013 km<sup>2</sup> within the Holtedahlfonna ice field (Bennett et al. 1999).

## Methods

The data presented come from three sampling periods: (i) July 2002 (cruise JR75) (ii) September 2005 (cruise JR127), both onboard RRS *James Clark Ross*, and (iii) 30 March–3 April 2005, sampling from stations on the fast ice (see Fig. 1). Temperature ( $T$ ) and salinity ( $S$ ) profiles in the outer fjord were recorded with a ship-deployed Sea-Bird Electronics 911 plus conductivity-temperature-depth (SBE9/11+ CTD) system, from which the potential temperature ( $\theta$ ) was derived. Water for isotopic measurement and salinity calibration were collected using the rosette sampler on cruise JR75 (July 2002).

The inner fjord was sampled during cruise JR127 using small boats. Profiles of  $T$  and  $S$  were recorded at 16 stations with a hand-deployed SBE19 CTD; water column samples were collected using NIO water bottles and 16 samples of 'calved' glacier ice were collected from the surface. Winter profiles in the inner fjord were collected at four stations using a Seabird SBE19+ CTD deployed

through the sea ice. A Guildline Autosol 8400b salinometer (accuracy,  $\pm 0.002$ ) was used to calibrate CTD salinity data, and to determine the salinity of water samples and melted glacial ice.

To minimize isotopic contamination of the glacial ice samples, a surface layer of ice was chipped away prior to storage (at  $-1^\circ\text{C}$ ). Further precautions before melting and analysis included removing a further surface layer of ice and transferring the sample to air-tight 'triple-layered' plastic bags to prevent leakage and exchange with the atmospheric oxygen. The seawater and melted ice samples for  $\delta^{18}\text{O}$  were transferred to 200-ml glass bottles and double sealed with a PVC stopper and a screw cap. Oxygen isotope ratios were measured on a Finnegan Delta plus XP gas source mass spectrometer, coupled to a gas-bench II preparation system, at the School of Geography and Geosciences, University of St Andrews. The  $\delta^{18}\text{O}$  measurements are based on 1-ml volumes, determined via  $\text{CO}_2$  equilibration. The mean precision of the triplicate analysis was  $\pm 0.04\text{‰}$  relative to Vienna Standard Mean Ocean Water (VSMOW). Four samples were measured in triplicate and two internal standard waters (calibrated to VSMOW) were analysed every ten samples.

## Results

Figures 2a and b show the potential temperature and salinity sections for the inner fjord derived from individual CTD profiles in September 2005. The temperature section shows a cool surface layer of around  $1.5^\circ\text{C}$  or less, with a gradual increase in temperature with distance from the glacier. There is a sharp thermocline at about 5 m, with temperature increasing to a maximum of nearly  $3^\circ\text{C}$  at approximately 10 m and then gradual cooling with depth. Stations IK1 and IK2 show a greater rate of cooling below 60 m depth.

The salinity section does not show a clear meltwater plume with associated large longitudinal salinity gradients within the inner fjord. Rather, isohalines in the surface layer at depths shallower than the sill (0–10 m) at IK9 maintain a relatively constant depth with a relatively weak longitudinal salinity gradient of  $0.02\text{ m}^{-1}$ . At the stations closest to the glacier front (IK2–IK8) there is a relatively weak vertical salinity gradient of  $0.025\text{ m}^{-1}$  at depths below the level of the sill at IK9, between isohalines 33 and 34. In contrast seaward of the sill at IK9 the corresponding vertical gradient is, salinity  $0.1\text{ m}^{-1}$ , four times greater than the gradient closer to the Glacier. The 34 isohaline lies at a depth of approximately 50 m between stations IK2 and IK4, compared with a depth of 20 m between IK11 and IK16.

Figure 3 is a potential temperature versus salinity ( $\theta$ – $S$ ) diagram comparing CTD data from April 2005 with data

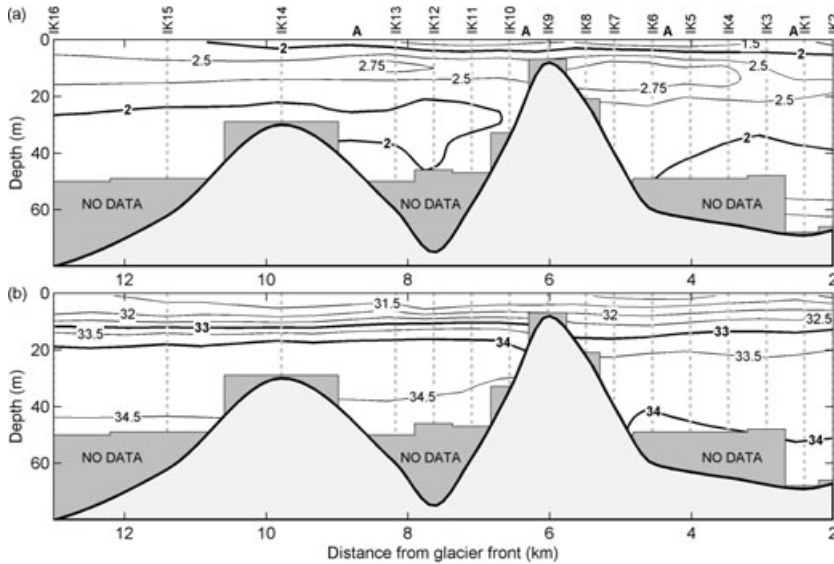


**Fig. 2** Sections of (a) potential temperature and (b) salinity in the inner fjord. Bathymetry is estimated from CTD drops and charts. Station locations are indicated by the vertical dashed lines. 'A' indicates the approximate placement of the April stations along the transect line. Isotherms are plotted at 1.0, 1.5, 2.0, 2.5 and 2.75°C and isohalines at 0.5 intervals between 31 and 34.5.

**Table 1** Details of  $\delta^{18}\text{O}\text{‰}$  (relative to Vienna Standard Mean Ocean Water, VSMOW) and salinity data obtained for Kongsfjorden.

	Precipitation <sup>a</sup>	Inner fjord (JR127)			Outer fjord (JR75)	
	1990–2002	Glacial ice	Surface water (0–2 m)	Deep water (>2 m)	Transformed AW <sup>b</sup> (6–52 m)	AW <sup>b</sup> (76–354 m)
Range of $\delta^{18}\text{O}$	from –5.23 to –26.58	from –14.62 to –17.96	from –1.00 to –1.47	from –0.02 to 0.21	from 0.06 to 0.40	from 0.13 to 0.51
Mean of $\delta^{18}\text{O}$	–11.55	–15.85	–1.22	0.10	0.20	0.24
Salinity range	0	0	from 30.23 to 31.60	from 33.53 to 34.23	from 34.02 to 34.59	from 34.66 to 35.14
Mean salinity	0	0	30.95	33.97	34.43	34.86
No. of samples	152	16	12	4	7	13

<sup>a</sup>Precipitation values extracted from IAEA (2006).

<sup>b</sup>Atlantic water.

from September 2005. A description of each water mass domain identified in Fig. 3 is given by Svendsen et al. (2002). In April the water in the inner fjord was rather homogeneous in temperature and salinity, which is consistent with the characteristics of winter cooled water (WCW), formed through sea-ice formation and convection, and described previously by Cottier et al. (2005). This affirms previous speculation that the entire body of water in Kongsfjorden becomes relatively homogeneous during the winter.

The large scatter in the September 2005 data in Fig. 3 is confined to the upper 12–15 m, with the  $\theta$ – $S$  relationship becoming rather well defined at salinities greater than 33. Towards the glacier front the water becomes uniformly cooler and more saline with depth, indicative of diffusive vertical mixing, with a trend towards a  $\theta$ – $S$  signature typical of WCW, which may persist in the deep water from the preceding winter. Seaward of the sill at IK9 the salinity also increases with depth, and remains rather warm. At 50 m the water is relatively uniform in charac-

ter with  $\theta \cong 2^\circ\text{C}$  and  $S \cong 34.5$ , a salinity value that exceeds those measured in April 2005.

The September 2005  $\delta^{18}\text{O}$  data (Table 1) show that the surface waters in the inner fjord are isotopically lighter than the deeper waters, with surface values ranging from –1.00‰ to –1.47‰, contrasting with a range from –0.02‰ to 0.21‰ for deep waters. Similarly to the weak surface salinity gradient (Fig. 2b), there is a weak horizontal gradient in surface  $\delta^{18}\text{O}$  that increases seaward at  $0.012\text{‰ km}^{-1}$ .  $\delta^{18}\text{O}$  values increase quickly with depth such that the  $\delta^{18}\text{O}$  mean at a depth of approximately 35 m adjacent to the glacier front is  $0.05\text{‰}$ . The Outer Fjord data generally shows higher  $\delta^{18}\text{O}$  values, varying from  $0.06\text{‰}$  to  $0.51\text{‰}$ , corresponding to the higher salinities (see Table 1).

Glacial ice was collected from IK2 to IK16 in the inner fjord. The  $\delta^{18}\text{O}$  values of these samples ranged from –14.62‰ to –17.96‰, with a mean of –15.85‰. The 3.34‰ isotopic variation in the ice samples analysed is comparable with that published for Svalbard ice-core data

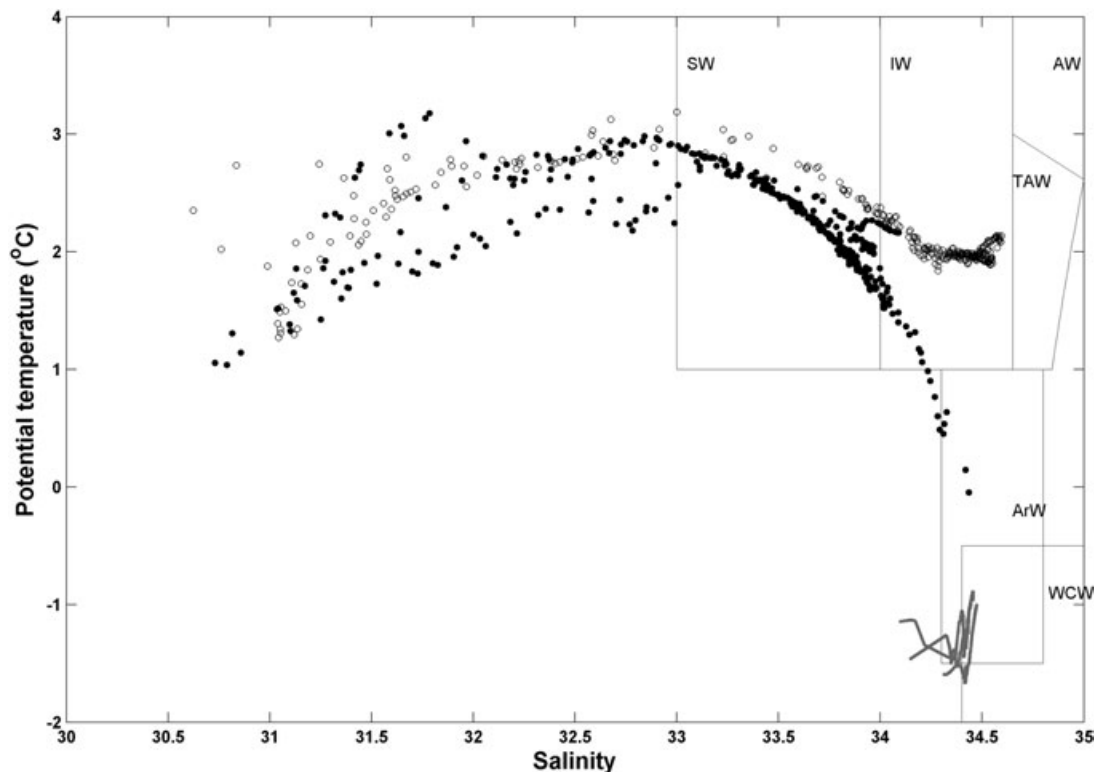


**Fig. 3** A potential temperature ( $\theta$ )–salinity ( $S$ ) diagram of CTD data collected in the inner fjord area in April 2005 (grey lines) and September 2005 (circles). Data from stations between IK2 and IK8 are denoted by filled circles and data from stations seaward from the sill at IK9 are denoted by open circles. Water mass boundaries are taken from Cottier et al. (2005). External water masses are Atlantic water (AW) and Arctic water (ArW); internal water masses are winter cooled water (WCW) and surface water (SW); water masses of mixed origin are transformed Atlantic water (TAW) and intermediate water (IW).

(e.g. Isaksson et al. 2003). Such variation can be attributed to (i) variations in the age and hence  $\delta^{18}\text{O}$  of the ice, (ii) varying altitude at which the ice was formed, and (iii) the ice originating from any one of the five tide water glaciers that discharge into the fjord.

The stable oxygen isotope composition of meteoric precipitation is primarily dependent upon the ambient local temperature. As local temperature varies with season, we have obtained monthly precipitation data from Ny-Ålesund (IAEA 2006) for 1990–2002 (Table 1). During this period, values for  $\delta^{18}\text{O}$  of precipitation varied from  $-5.23\text{‰}$  (October 2002) to  $-22.93\text{‰}$  (February 1995) with a mean of  $-11.55\text{‰}$ . It is worth noting that a significant component of winter precipitation (October–March) within the catchment has the potential to influence the fjord  $\delta^{18}\text{O}$  as snowmelt.

## Discussion

Figures 2 and 3 illustrate the complex hydrography and the possible modification processes occurring in the inner

fjord. The occurrence of predominantly WCW in the April CTD data shown in Fig. 3 is a strong indicator that input of meltwater was minimal at that time. By September, two major modifications to the salinity distribution have taken place. First, a fresh surface layer developed, through summer melt and run-off. Second, there was apparent uplift of the 34 isohaline to a depth of 20 m seaward of the sill at IK9 in the inner fjord, which was probably caused by a subsurface intrusion of a more saline water mass.

The primary source of saline water in this system is AW originating in the WSC. The occurrence of heavily modified AW, through mixing, in Kongsfjorden has been described by Svendsen et al. (2002) and was termed transformed Atlantic water (TAW). Figure 3 confirms that there is a greater influence of AW on the seaward side of the sill at IK9, with the deep water tending towards the TAW domain. However, the inflection in the  $\theta$ – $S$  distribution towards TAW implies that AW is not restricted to the seaward side, but is also present closer to the glacier, although heavily mixed with the surface

water and the WCW. The cool surface layer and temperature maximum at 10 m (Fig. 2a) can be interpreted as previous warming of the surface through insolation, followed by a recent cooling by cold down-fjord winds.

The summer salinity structure close to a glacier is often characterized by a freshwater plume (Domack & Ishman 1993). From the vertical and horizontal salinity gradients in Fig. 2 there was no discernible subsurface plume in Kongsfjorden in September 2005. Furthermore, the observed contrast between  $\delta^{18}\text{O}$  values at the surface and those at depth (Fig. 4a) reinforces the assertion that melt-water is restricted to the upper 15 m. The absence of a subsurface plume may be accounted for by the following: (i) the first station was approximately 2 km from the glacier front, and a buoyant plume ascending the face of the glacier could mix with ambient water with only a fresher surface layer detectable at the first station; also (ii) the cyclonic circulation in Kongsfjorden (Ingvaldsen et al. 2001) will tend to cause freshwater to flow to the northern side of the fjord rather than form a uniform axial plume. However, the sampling line is to the north of Kongsvegen and therefore is likely to intersect a northward flowing subsurface plume. A similar absence of a subsurface plume has also been reported in an East Greenland fjord (Azetsu-Scott & Tan 1997).

The salinity and isotope data for inner fjord seawater, collected in September 2005, are presented in Fig. 4a as a salinity:  $\delta^{18}\text{O}_{\text{water}}$  mixing line. It spans both the fresh surface water and those deeper waters with a stronger Atlantic influence. The mixing line has a gradient of 0.42‰ per salinity unit with an intercept value at  $S = 0$  of  $-14.35\text{‰}$ . We are also able to make an independent esti-

mate of the zero salinity value using published data of monthly freshwater discharge into Kongsfjorden from glacial and precipitation sources. Svendsen et al. (2002: table 3) estimate that the total glacial source including icebergs is  $1016 \times 10^6 \text{ m}^3$ , and from precipitation is  $377 \times 10^6 \text{ m}^3$ , a volume ratio of 2.7 : 1. Using  $\delta^{18}\text{O}$  values of  $-15.85\text{‰}$  for glacial ice and  $-11.55\text{‰}$  for precipitation (Table 1), and by combining them at the appropriate volume ratio we derive a freshwater end member of  $-14.69\text{‰}$ . Within the errors associated with the discharge data this is remarkably close to the intercept obtained in Fig. 4a (i.e.  $-14.35\text{‰}$ ) and offers a level of confirmation of the Svendsen et al. (2002) data. We will use  $-14.69\text{‰}$  as our freshwater end member.

We can extend the mixing line of Fig. 4b to include data from two central and outer stations, which are more influenced by AW (Cottier et al. 2005), and force it through the derived freshwater end member. The calculated mixing line presented in Fig. 4b shows that the data can be fitted to a line with equation  $\delta^{18}\text{O} = 0.43S - 14.69$ . This robust mixing line can be used for all areas of the fjord because of the strong linear relationship that connects the variety of mixed water masses encountered. Furthermore, none of the data points deviate significantly from the mixing line towards higher or lower salinities at constant  $\delta^{18}\text{O}$  values, indicating that neither sea-ice formation (with associated brine release) nor sea-ice melt, respectively, make a significant contribution to the surface salinity (Bedard et al. 1981) in Kongsfjorden.

A similar investigation was undertaken by Azetsu-Scott & Tan (1997) in Kangerlugssuaq Fjord, eastern Greenland. A salinity:  $\delta^{18}\text{O}$  relationship of  $\delta^{18}\text{O} = 0.69S - 24.18$

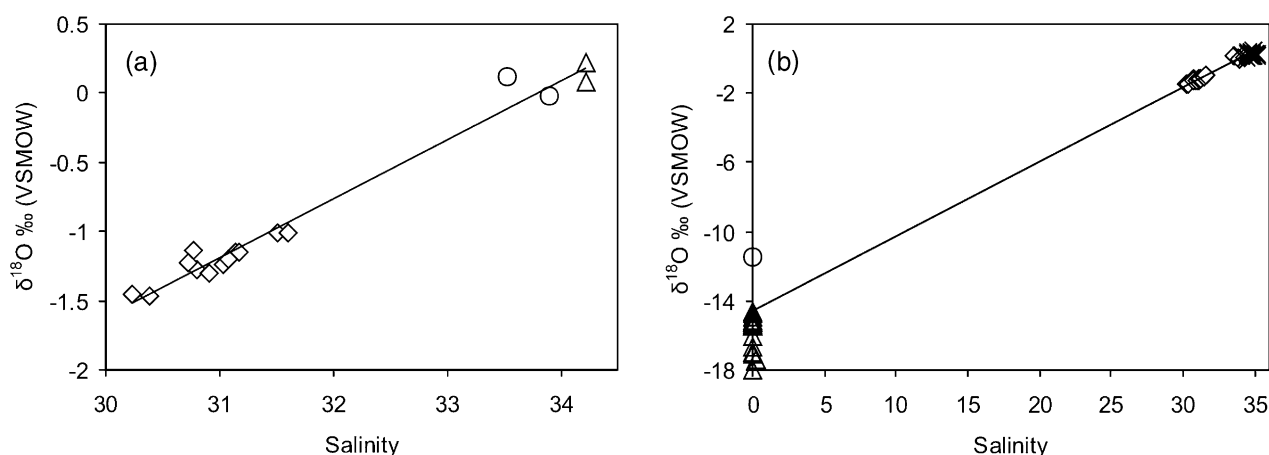


**Fig. 4** (a) Salinity:  $\delta^{18}\text{O}$  mixing line, Inner Fjord, September 2005 ( $n = 16$ ).  $\delta^{18}\text{O}_{\text{water}} = 0.42S - 14.35$  ( $R^2 = 0.977$ ). Data points are denoted by open diamonds for surface water, open circles for intermediate depth samples and open triangles for bottom water samples. (b) Salinity:  $\delta^{18}\text{O}$  mixing line, Kongsfjorden, July 2002 and September 2005 ( $n = 53$ ).  $\delta^{18}\text{O}_{\text{water}} = 0.43S - 14.69$  ( $R^2 = 0.982$ ). Data points are denoted by open diamonds for inner fjord samples, an open circle for mean meteoric value open triangles for glacial ice samples and crosses for outer fjord samples.

was calculated for the inner fjord. The slope of the Kangerlugssuaq mixing line (0.69) is much greater than that for the inner Kongsfjorden mixing line (0.43) because of the isotopic differences in the glacier ice at the head of the fjords. For instance, the glacial ice sampled from Kangerlugssuaq Fjord yielded an isotopic mean of  $-26.5\text{‰}$ , in comparison with  $-15.85\text{‰}$  for Kongsfjorden.

The Kongsfjorden data provide a northern latitudinal limit for mixing lines in the north-western European coastal system. To set our results in the context of other fjordic locations that have a strong freshwater input and an AW influence, we compare our mixing line with those derived for Loch Sunart, Scotland ( $57^\circ\text{N}$ ) (Austin & Inall 2002) and Sognefjorden, Norway ( $61^\circ\text{N}$ ) (Mikalsen & Sejrup 2000) in Fig. 5. The three sites lie on a latitudinal gradient, along which there is a supply of AW and a marked variation in the freshwater oxygen isotope signal. As anticipated, the slope of the mixing line in Fig. 4b (0.43) is greater than relationships defined for Sognefjorden, western Norway (0.31) and Loch Sunart, western Scotland (0.18). This spatial gradient in the salinity:  $\delta^{18}\text{O}$  mixing lines occurs as a result of the latitudinal effect of  $\delta^{18}\text{O}$  in precipitation (see Austin and Inall 2002).

Variations in both salinity and temperature have the potential to be imprinted in the palaeoclimate record of marine organisms. Consequently, it is crucial to identify the factors (both spatial and temporal) governing  $\delta^{18}\text{O}$  within the fjordic environment. The relationship between salinity and  $\delta^{18}\text{O}$  illustrated in Fig. 5 will be a valuable tool in palaeoceanographic research, particularly with respect to palaeotemperature reconstructions from Arctic fjords.

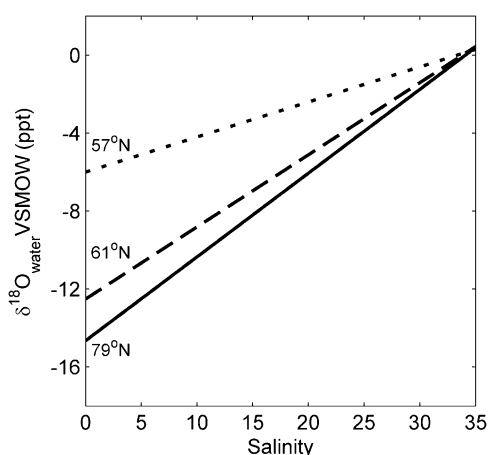


**Fig. 5** Salinity:  $\delta^{18}\text{O}$  mixing lines:  $57^\circ\text{N}$  Loch Sunart, western Scotland,  $\delta^{18}\text{O}_{\text{water}} = 0.185 - 6.0$  (Austin & Inall, 2002);  $61^\circ\text{N}$  Sognefjorden, western Norway,  $\delta^{18}\text{O}_{\text{water}} = 0.375 - 12.51$  (Mikalsen & Sejrup 2000); and  $79^\circ\text{N}$  Kongsfjorden, western Svalbard,  $\delta^{18}\text{O}_{\text{water}} = 0.435 - 14.65$ .

## Conclusions

The combined hydrographic and isotopic data presented yield the first salinity:  $\delta^{18}\text{O}$  mixing line for the fjordic and coastal waters of western Svalbard, a key high-latitude oceanographic province strongly influenced by both glacial melt and AW. We also provide the first reports of seasonal evolution of the inner fjord hydrography, showing that the influence of AW extends throughout the fjord. We demonstrate that despite the hydrographic complexity of Kongsfjorden, a robust salinity:  $\delta^{18}\text{O}$  relationship exists, confirming the utility of oxygen isotopes as a tool for studying the complex relationship between water masses in an Arctic environment. The resulting salinity:  $\delta^{18}\text{O}$  relationship confirms that the freshwater input to the fjord is dominated by glacial melt from the Holtedahlfonna ice field, rather than by seasonal precipitation or sea-ice melt.

The derived salinity:  $\delta^{18}\text{O}$  relationship provides a new palaeoceanographic proxy calibration for the region. The mixing line for Kongsfjorden is a northern extreme for the fjordic north-western European coastal system. We regard the mixing line as a valid palaeoclimate tool for western Svalbard fjords, and recommend its application in future palaeoclimate studies from the region, particularly those concerned with the present (Holocene) interglacial period.

## Acknowledgements

We thank the officers and crew of RSS *James Clark Ross* during the 2002 and 2005 cruises; also Edmond Hansen (Norwegian Polar Institute) for supplying the April 2005 CTD data. Colin Griffiths and Paul Provost (Scottish Association for Marine Science) are thanked for their help with CTD operations, sample collection and salinity measurements. Jonathan Wynn (School of Geography and Geosciences, University of St Andrews) is thanked for his help with stable isotope measurements.

## References

- Austin W.E.N. & Inall M.E. 2002. Deep-water renewal in a Scottish fjord: temperature, salinity and oxygen isotopes. *Polar Research* 21, 251–257.
- Azetsu-Scott K. & Tan F.C. 1997. Oxygen isotope studies from Iceland to an East Greenland Fjord: Behaviour of glacial meltwater plume. *Marine Chemistry* 56, 239–251.
- Bauch D., Erlenkeuser H. & Andersen N. 2005. Water mass processes on Arctic shelves as revealed from delta O-18 of H2O. *Global and Planetary Change* 48, 165–174.
- Bauch D., Schlosser P. & Fairbanks R.G. 1995. Freshwater balance and the sources of deep and bottom waters in the

- Arctic Ocean inferred from the distribution of  $\text{H}_2^{18}\text{O}$ . *Progress of Oceanography* 35, 53–80.
- Bedard P., Hillaire-Marcel C. & Page C. 1981.  $^{18}\text{O}$  modelling of freshwater inputs in Baffin Bay and Canadian Arctic coastal waters. *Nature* 293, 287–289.
- Bennett M.R., Hambrey M.J., Huddart D., Glasser N.F. & Crawford K. 1999. The landform and sediment assemblage produced by a tidewater glacier surge in Kongsfjorden, Svalbard. *Quaternary Science Reviews* 18, 1213–1246.
- Cottier F., Tverberg V., Inall M. E., Svendsen H., Nilsen F. & Griffiths C. 2005. Water mass modification in an Arctic fjord through cross-shelf exchange: the seasonal hydrography of Kongsfjorden, Svalbard. *Journal of Geophysical Research, Oceans* 110, 1–18.
- Craig H. & Gordon L. 1965. Deuterium and oxygen-18 variations in the ocean and the marine atmosphere. In E. Tongioli (ed.): *Stable isotopes on oceanographic studies and paleotemperatures*. Pp. 9–130. Pisa: National Research Council.
- Domack E.W. & Ishman S. 1993. Oceanographic and physiographic controls on modern sedimentation within Antarctic fjords. *Geological Society of America Bulletin* 105, 1175–1189.
- Freeland H.J., Farmer D.M. & Levings C.D. (eds.) 1980. *Fjord oceanography*. *NATO Conference Series*, 715. New York/London: Plenum Press.
- Howe J. A., Moreton S. G., Morri C. & Morris P. 2004. Multi-beam bathymetry and the depositional environments of Kongsfjorden and Krossfjorden, western Spitsbergen, Svalbard. *Polar Research* 22, 301–316.
- IAEA (International Atomic Energy Agency) 2006. *The Global Network of Isotopes in Precipitation (GNIP) and Isotope Hydrology Information System (ISOHIS) Database*. Vienna: IAEA.
- Ingvaldsen R., Bø-Reitan M., Svendsen H. & Asplin L. 2001. The upper layer circulation in the Kongsfjorden and Krossfjorden—a complex fjord system on the west coast of Spitsbergen. Watanabe O. & Yamanouchi T. (eds.) *Environmental Research in the Arctic 2000: Proceedings of the Second International Symposium on Environmental Research in the Arctic and fifth Ny-Ålesund Scientific Seminar*. *Memoirs of National Institute of Polar Research Special issue* 54, 393–407. Tokyo: National Institute of Polar Research.
- Isaksson E., Hermanson M., Hicks S., Igarashi M., Kamiyama K., Moore J., Motoyama H., Muir D., Pohjola V., Vaikmae R., van der Wal R. S. W. & Watanabe O. 2003. Ice cores from Svalbard—useful archives of past climate and pollution history. *Physics and Chemistry of the Earth* 28, 1217–1228.
- Ito H. & Kudho S. 1997. Characteristics of water in Kongsfjorden, Svalbard. *Proceedings of the NIPR Symposium, Polar Meteorology Glaciology* 11, 211–232. Tokyo: National Institute of Polar Research.
- Jansen E. 1989. The use of stable oxygen isotope and carbon isotope stratigraphy as a dating tool. *Quaternary International* 1, 151–166.
- Mikalsen G. & Sejrup H.P. 2000. Oxygen isotope composition of fjord and river water in the Sognefjorden drainage area, western Norway. Implications for paleoclimate studies. *Estuarine and Coastal Marine Science* 50, 441–448.
- Saloranta T.M. & Svendsen H. 2001. Across the Arctic front west of Spitsbergen: High-resolution CTD sections from 1998–2000. *Polar Research* 20, 177–184.
- Schauer U., Fahrbach E., Østerhus S. & Rohardt G. 2004. Arctic warming through the Fram Strait: oceanic heat transport from 3 years of measurements. *Journal of Geophysical Research* 109, Article Number C06026. doi:10.1029/2003JC001823.
- Svendsen H., Beszczynska-Møller A., Hagen J. O., Lefauconnier B., Tverberg V., Gerland S., Ørbæk J. B., Bischof K., Papucci C., Zajaczkowski M., Wiencke C., Winther J.-G. & Dallmann W. 2002. The physical environment of Kongsfjorden–Krossfjorden, an Arctic fjord system in Svalbard. *Polar Research* 21, 133–166.
- Syvitski J.P., Burrell D.C. & Skei J. (eds.) 1984. *Fjords: processes and products*. New York: Springer Verlag.
- Willis K., Cottier F., Kwasniewski S., Wold A. & Falk-Petersen S. 2006. The influence of advection on zooplankton community composition in an Arctic fjord (Kongsfjorden, Svalbard). *Journal of Marine Systems* 61, 39–54.